Turkish Journal of Physics

Volume 36 | Number 3 Article 4

1-1-2012

# Admixture of higher multi-\hbar\omega configurations in the calculation of electron scattering form factors of some 1p-shell nuclei

AMMAR A. AL-SA'AD

TÜBİTAK

Turk J Phys
36 (2012) , 352 – 360.

doi:10.3906/fiz-1110-1

# Admixture of higher multi-$\hbar\omega$ configurations in the calculation of electron scattering form factors of some 1p-shell nuclei

**Ammar A. AL-SAAD**
*Department of Physics, College of Science, University of Basrah, Basrah-IRAQ*
*e-mail: ammarlsd@yahoo.com*

Received: 02.10.2011

**Abstract**

A semi-microscopic approach that modifies the 1p-shell model wave functions through the admixture of higher p-shells configurations from multi-$\hbar\omega$ model space is submitted in this work. The longitudinal form factors of C2 transitions in $^{7}$Li and $^{15}$N, and the transverse form factors of M1 transition in $^{12}$C are calculated in the framework of this approach with the emphasis on the reproduction of the second lobe data. It is found that a slight contribution of the higher multi-p-shells with the 1p-shell in the modified initial and/or final states wave functions is sufficient for giving the best description to the form factors data.

**Key Words:** C2 and M1 form factors, incomplete multi-$\hbar\omega$ model space

## 1. Introduction

Electron scattering is a very valuable tool for testing the nuclear models wave functions. For the conventional 1p-shell model of Cohen and Kurath (CK-model) [1], the interaction included was determined in the smallest model space possible for the nuclei of this region (0 $\hbar\omega$ model space). The extracted CK-model wave functions are appropriate for calculating the observable quantities that depend on the 1p-shell nature, such as magnetic dipole moments, Gamow-Teller (GT) $\beta$-decay and M1 $\gamma$-transitions, but they fail in describing the electron scattering form factors at high momentum transfer [1]. This deficiency is attributed to the truncation of the space which is restricted to the $1p_{3/2}$ and $1p_{1/2}$ shells, only.

Wolters et al. [2] develop an empirical effective interaction for 1p-shell nuclei in the complete $(0+2)\hbar\omega$ model space, which is shown to be quite successful for energies, static moments and transition rates. They found that an extension of the model space from $0\hbar\omega$ to $(0+2)\hbar\omega$ does not considerably improve the calculated form factors [3], and they ascribed the discrepancy between the theoretical and experimental form factors to the need for larger than $(0+2)\hbar\omega$ model space or relativistic and/or mesonic effects. Towards the end of the p-shell, Booten and van Hees [4] found that meson exchange currents (MECs) could only partly cure the deficiencies in the wave functions, and thus they confirm the need for components other than $(0+2)\hbar\omega$.

To make benefit of the 1p-shell model ($0\hbar\omega$) wave functions in the reproduction of the form factors data, the truncated space can be compensated by combining the 1p-shell model wave functions with highly-excited states by using first order perturbation theory. This approach is called core polarization effect. Radhi et al. [5] use such an approach to study the C2 form factors of 1p-shell nuclei. In spite of their remarkably good agreement with measured data, core polarization effects in this study fail to reproduce the diffractive structure of $^{7}$Li data at high momentum transfer values and they left it as an open question to be studied.

The truncation of the model space can be reformed in another way that makes use of the independence of the CK interaction from the radial wave function of the single-particle states, which is the modification of the model space in such a way that combines 1p and 2p shells. This approach is argued by Talmi [6] following the use of Huffman et al. [7] phenomenological wave functions to calculate the form factors of $^{14}$N. Such an extension in the model space that mixes 1p+2p shells is used by Radhi et al. [8] to explain the diffractive structure of the elastic magnetic electron scattering from $^{19}$F. This extension is enlarged in the present work to include the mixing of (1p + 2p + $\cdots$ + $n$p) configurations in order to give the best description for the form factors at high-q values.

## 2. Theory

Electron scattering form factors involving angular momentum $J$, isospin $T$ and momentum transfer $q$, between the initial and final nuclear shell model states of spin $J_{i,f}$ and isospin $T_{i,f}$, are described by [9]

$$\left|F_J^{L,m}(q)\right|^2 = \frac{4\pi}{Z^2(2J_i+1)}\left|\sum_{T=0,1}\begin{pmatrix} T_f & T & T_i \\ -T_z & 0 & T_z \end{pmatrix}\left\langle J_fT_f\left\|\left|T_{JT}^{L,m}(q)\right|\right\|J_iT_i\right\rangle\right|^2 |F_{fs}(q)|^2\,|F_{cm}(q)|^2\,, \quad (1)$$

where $T_z$ is the z-component of the isospin for the initial and final states and is given by $T_z=(Z-N)/2$. $F_{fs}(q)$ and $F_{cm}(q)$ are respectively, the corrections for the finite-nucleon size, $\exp\left(-0.43q^2/4\right)$, and the center-of-mass motion, $\exp\left(b^2q^2/(4A)\right)$ [10]. Here, $Z$, $b$ and $A$ are the atomic number, size parameter and mass number, respectively. The reduced many-body matrix elements for shell-model wave functions of initial and final spin $\boldsymbol{J}_{i,f}$ and isospin $\boldsymbol{T}_{i,f}$ can be expressed as a linear combination of the reduced single-particle matrix elements [9]

$$\left\langle J_fT_f\left\|\left|T_{JT}^{L,m}(q)\right|\right\|J_iT_i\right\rangle = \sum_{j_ij_f} OBDM(J_i,T_i,J_f,T_f,J,T,j_i,j_f)\left\langle j_ft_f\left\|\left|T_{JT}^{L,m}(q)\right|\right\|j_it_i\right\rangle, \quad (2)$$

with the electron scattering operators $T_J^{L,m}(q)$ are either $T_J^L(q)$ for longitudinal transition or $T_J^m(q)$ for transverse magnetic transition.

The single-particle matrix element that is reduced in both spin and isospin is written in terms of that reduced in spin only [9]:

$$\left\langle j_ft_f\left\|\left|T_{JT}^{L,m}(q)\right|\right\|j_it_i\right\rangle = \sqrt{\frac{2T+1}{2}}\sum_{t_z} I_T(t_z)\left\langle j_f\left\|T_{Jt_z}^{L,m}(q)\right\|j_i\right\rangle, \quad (3)$$

where $I_T(t_z) = \begin{cases} 1 & \text{for} \quad T=0 \\ (-1)^{1/2-t_z} & \text{for} \quad T=1 \end{cases}$, and $t_z$ = 1/2 for proton and -1/2 for neutron. The reduced

single-particle matrix elements of the electron scattering operators are given explicitly by Brown et al. [11]. The one-body density matrix elements, OBDM, which contain the complexities of nuclear structure, are given by Lee and Kurath [12] for the 1p-shell nuclei.

Writing the initial and final single-particle states $|i\rangle \equiv |j_i\rangle$ and $|f\rangle \equiv |j_f\rangle$ by replacing them with the following linear combinations of single-particle basis that keep the angular part unchanged, brings

$$|i\rangle = \sum_{k=0}^{n} \alpha_k \left| n_i^{(k)} \ell_i j_i \right\rangle, \tag{4a}$$

$$|f\rangle = \sum_{k'=0}^{n} \beta_{k'} \left| n_f^{(k')} \ell_f j_f \right\rangle, \tag{4b}$$

where amplitudes $\alpha_k$ and $\beta_{k'}$ are taken as free parameters that satisfy the orthonormality conditions $\sum\limits_{k=0} |\alpha_k|^2 = 1$ and $\sum\limits_{k'=0} |\beta_{k'}|^2 = 1$, respectively. Also, the radial quantum number of the initial and final states are changed to $n_i^{(k)} = 1 + k$ and $n_f^{(k')} = 1 + k'$, respectively.

The expansion of the initial and final states given in equations (4) mixes p-shell configurations from multi-$\hbar\omega$ spaces with that of $0\hbar\omega$, i.e. mixes the higher-energy orbits (2p + 3p + $\cdots$ + np) with the 1p shell. In other word, the present work submits a calculation method for the form factors in an incomplete multi-$\hbar\omega$ model space since it neglects many other configurations but the p shells. However, this simple modification in the wave functions enables us to calculate the reduced many-particle matrix elements by using the OBDM elements of the 1p-shell model as they are independent of the principal quantum number. The use of equations (4) modifies the reduced single-particle matrix elements to

$$\left\langle j_f \left\| T_{Jt_z}^{L,m}(q) \right\| j_i \right\rangle = \sum_{kk'} \alpha_k \beta_{k'} \left\langle n_f^{(k')} \ell_f j_f \left\| T_{Jt_z}^{L,m}(q) \right\| n_i^{(k)} \ell_i j_i \right\rangle. \tag{5}$$

## 3. Results and discussion

The one-body density matrix elements (OBDM) of the 1p-shell model are used in calculations of the form factors of electron scattering from the p-shell nuclei $^7$Li, $^{12}$C, and $^{15}$N in a large extended space which include admixture from higher multi-$\hbar\omega$ p-shell configurations. The reduced single-particle matrix elements of the electron scattering operators are calculated according to equation (5). Thus, the OBDM elements of 1p-shell model, which convert the single-particle calculations to a many-particle calculation, are modified by the product of the parameters $\alpha_k$ and $\beta_{k'}$ for each higher p-shell that admixed with the 1p-shell. These parameters are taken as adjustable parameters that reproduce the best description of the form factors data, and the only correlation among them is the orthonormality conditions of the extended initial and final states. The size parameters, $b$, of the harmonic oscillator single-particle wave functions employed in this work are 1.77 [13], 1.64 [14] and 1.678 fm [15], that reproduce the root-mean-square charge distribution of $^7$Li, $^{12}$C and $^{15}$N, respectively.

The reduced transition probabilities at the photon point $B(C2\uparrow, k)$ and $B(M1\uparrow, k)$ where $k = \frac{Ex}{\hbar c}$, are calculated from $\left|F_{J=2}^{L}(k)\right|^2$ and $|F_{J=1}^{m}(k)|^2$, respectively, according to Brown et al. [11].

### 3.1. $J^\pi T(E_X, MeV) = \frac{1}{2}^- \frac{1}{2}(0.478)$ and $\frac{7}{2}^- \frac{1}{2}(4.63)$ states in $^7$Li

The ground state of $^7$Li has $J^\pi T = \frac{3}{2}^- \frac{1}{2}$. The electro-excitation of $^7$Li from its ground state to those two states has prominent longitudinal C2 components. As shown in Figures 1 and 2, the experimental data show diffractive structure with two lobes separated by a minimum value around $q \approx 3\, fm^{-1}$. The dotted curves in both figures represent $0\hbar\omega$ model space (CK-model) calculations of the C2 form factors, which reproduce the shape of the first lobe only. Giving the valence nucleons effective charges, which have values different from free nucleons charges by the increment $\delta e = 0.35\, e$, the results enhance to be in very good agreement with the first lobe data. This procedure is due to core polarization effects (q-independent) and is shown in the dashed-dotted curves in both figures.

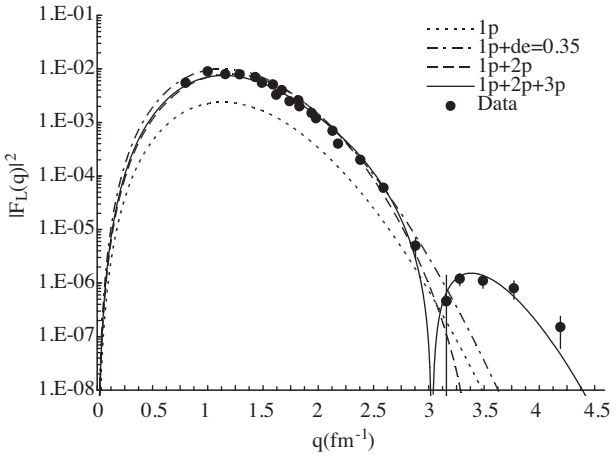


**Figure 1.** Longitudinal C2 form factor for $J^\pi, T = \frac{1}{2}^-, \frac{1}{2}$ state at $E_x$=0.478 MeV in $^7$**Li**. Data is from [18].

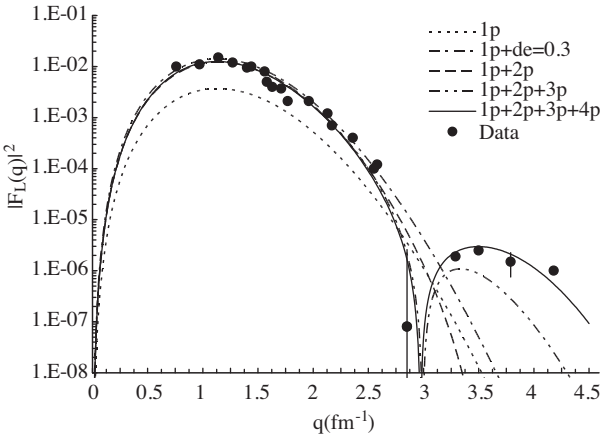


**Figure 2.** Longitudinal C2 form factor for $J^\pi, T = \frac{7}{2}^-, \frac{1}{2}$ state at $E_x$=4.63 MeV in $^7$**Li**. Data is from [19].

Calculations of 1p-shell model plus microscopic (q-dependent) core polarization effects that include higher-energy particle-hole excitations up to $6\,\hbar\omega$ [5] show analogous results to that displayed in the dashed-dotted curves of Figures 1 and 2, and fail to reproduce the data that follow the minimum diffractions. On the other hand, fully microscopic shell model calculations over the complete $(0+2)\,\hbar\omega$ [16] and $(0+2+4)\,\hbar\omega$ [17] model spaces fail, also, to reproduce these structures.

In the present calculations, an admixture of 2p shells with 1p shells, (1p+2p), in the initial and final states, shifted the first minima diffractions in both Figures 1 and 2 closer to the experimental responses, as shown in the dashed curves. While admixture of (1p+2p+3p) shells in the initial and final states succeeds in describing the C2 form factors data of the $\frac{1}{2}^- \frac{1}{2}$ state in $^7$Li, as shown in the solid curve of Figure 1.

These linear combinations of modified initial and final states are

$$|i\rangle = -0.975\,|1p\rangle + 0.1\,|2p\rangle + 0.198\,|3p\rangle\,,$$

$$|f\rangle = 0.95\,|1p\rangle + 0.1\,|2p\rangle + 0.296\,|3p\rangle\,.$$

The somewhat broad peak beyond $q \approx 3\, fm^{-1}$ of the C2 form factors of $\frac{7}{2}^- \frac{1}{2}$ state in $^7$Li cannot be reproduced by such an admixture of p shells, as shown in the dashed-double dotted curve of Figure 2. However, this state

requires admixture of (1p+2p+3p+4p) shells in the initial and final states,

$$|i\rangle = -0.98\,|1p\rangle + 0.09\,|2p\rangle + 0.07\,|3p\rangle + 0.163\,|4p\rangle\,,$$

$$|f\rangle = 0.98\,|1p\rangle + 0.09\,|2p\rangle + 0.07\,|3p\rangle + 0.163\,|4p\rangle\,,$$

to enhance the resulting C2 form factor, and is shown as a solid curve in Figure 2. The above wave functions denote directly that our calculations are carried out in incomplete $(0+2+4)\,\hbar\omega$ and $(0+2+4+6)\,\hbar\omega$ model spaces.

On the other hand, the transition strengths at the photon point $B(C2\uparrow, q=k)$ are enhanced by introducing the effective charges only. But there, values deteriorate as admixtures of higher p shells are taken into account, as shown in Table 1.

**Table 1.** Theoretical values of reduced transition probabilities $B(C2\uparrow,k)$ (in units of $e^2\ fm^4$) and $B(M1\uparrow,k)$ (in units of $\mu_N^2$) in comparison with the experimental values.

| Nucl. | $J_f^\pi$ | $T_f$ | $E_X^{(a)}$ | $mJ^{(b)}$ | 1p | $+\delta$e:$\delta g_s$ | +2p | +3p | +4p | +5p | +6p | +7p | Exp. |
|---|---|---|---|---|---|---|---|---|---|---|---|---|---|
| $^7$Li | $1/2^-$ | 1/2 | 0.478 | C2 | 1.725 | 7.263 | 4.002 | 4.72 | | | | | 8.3 (0.5)$^{(c)}$ |
| $^7$Li | $7/2^-$ | 1/2 | 4.63 | C2 | 2.675 | 10.17 | 8.04 | 8.19 | 8.046 | | | | 15 (1.9)$^{(c)}$ |
| $^{12}$C | $1^+$ | 1 | 15.11 | M1 | 6.84 | 3.477 | 2.621 | 2.623 | 2.623 | 2.623 | 2.623 | 2.623 | 2.78 (0.08)$^{(d)}$ |
| $^{15}$N | $3/2^-$ | 1/2 | 6.32 | C2 | 7.88 | 13.33 | 9.28 | 9.45 | 13.22 | 13.21 | 13.13 | | 14.8 (??)$^{(e)}$ |

(a) Excitation energies are in MeV. (b) Multipolarity. (c) Ref. [20]. (d) Ref. [21]. (e) Ref. [22].

## 3.2. $J^\pi T\ (E_X,\ MeV) = 1^+1\ (15.11)$ state in $^{12}$C

The excitation of $^{12}$C from the ground state $(0^+0)$ to the excited state $(1^+1)$ is by isovector M1 transition. The higher precision experimental data of Deutschmann et al. [23] for M1 form factors are displayed as full circles in Figures 3 and 4. Using Cohen-Kurath wave functions and the effective operators by introducing the value $g_s$ (eff.) $= 0.72\,g_s$ (free) for valence protons and neutrons, cannot extract the correct experimental form factors, as shown in the dotted and dashed curves of Figure 3, respectively. The extension of the ground state (initial) wave function to include (1p+2p) shells reproduces the minimum diffraction at $q \approx 1.3\ fm^{-1}$ as well as the first lobe data. However, the admixture of 2p shell in our calculations underestimates the data after $q > 1.7\ fm^{-1}$. These results are shown as solid curve in Figure 3.

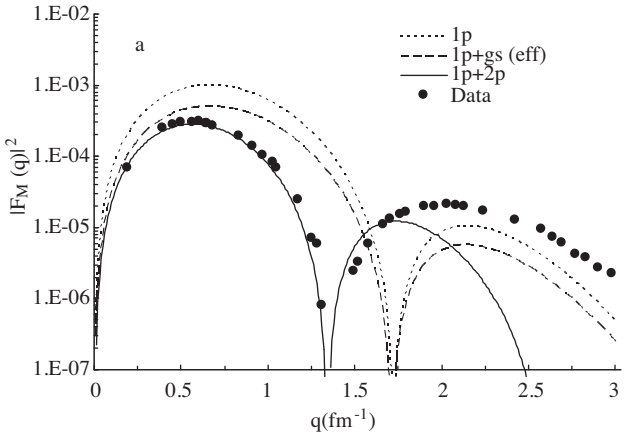


**Figure 3.** M1 form factor for $J^\pi, T = 1^+, 1$ state at 15.11 MeV in $^{12}$**C.** Data is from [20].

The transition to this state in $^{12}$C has been the subject of many previous studies. The suppression of CK model calculations as compared with the second lobe experimental data is enhanced significantly by taking into account the effects of the first order core polarization and meson exchange currents (MECs) [24]. In a calculation method similar to that of Reference [24], Suzuki et al. [25] follow another exchange characters for the central components of the residual interaction. Their calculations are fitted the data up to the peak of the second lobe and fall off like the solid curve of Figure 3.

The complete $(0+2)\,\hbar\omega$ model space calculations [26] for the transverse M1 form factors of this state as well as that including two-level isospin mixing underestimate all the data of the second lobe.

Figure 4 shows the results of the present work as compared with the experimental data. One can observe that the curves of the calculated M1 form factors of the second lobe are stretched as the number of higher shells that taken into account are increased. Finally, by introducing the $7^{th}$ p-shell in the modified initial wave function, the Deutschmann et al. data are reproduced excellently, as shown in the solid curve of Figure 4. This modified wave function is

$$\begin{aligned} |i\rangle = \quad & -0.87\,|1p\rangle + 0.38\,|2p\rangle + 0.024\,|3p\rangle + 0.024\,|4p\rangle \\ & +0.024\,|5p\rangle + 0.2\,|6p\rangle + 0.2387\,|7p\rangle\,. \end{aligned}$$

On the other hand, the use of this extended wave function reproduces a value for the reduced transition probability $B(M1\uparrow, q=k)$ to this state is less than the experimental one by 5.6% only as given in Table 1.

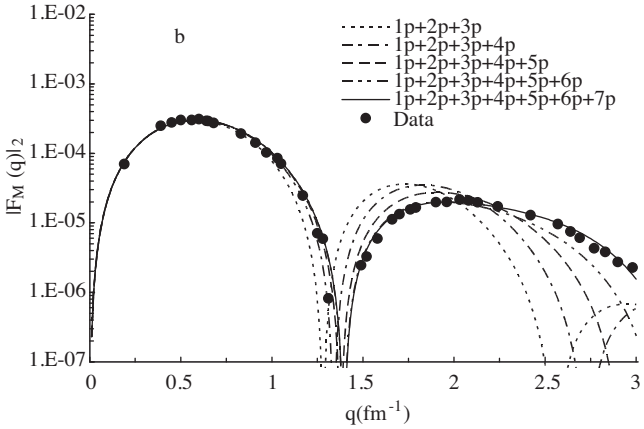


**Figure 4.** M1 form factor for $J^\pi, T = 1^+, 1$ state at 15.11 MeV in $^{12}$**C.** Data are from [20].

## 3.3. $J^\pi T(E_X, MeV) = \frac{3}{2}^-\frac{1}{2}(6.32)$ state in $^{15}$N

The experimental data of the C2 form factors of this state are displayed as full circles in Figures 5 and 6 show diffractive structure with minimum value at $q \approx 2.5\,fm^{-1}$. The C2 form factors that shown as dotted curve in Figure 5 are obtained by using Cohen-Kurath wave functions. The addition of effective charges to the valence protons and neutrons with $\delta e = 0.3e$ give the results that shown as the dashed curve in this figure. Both curves fail to show the diffractive behavior of the data.

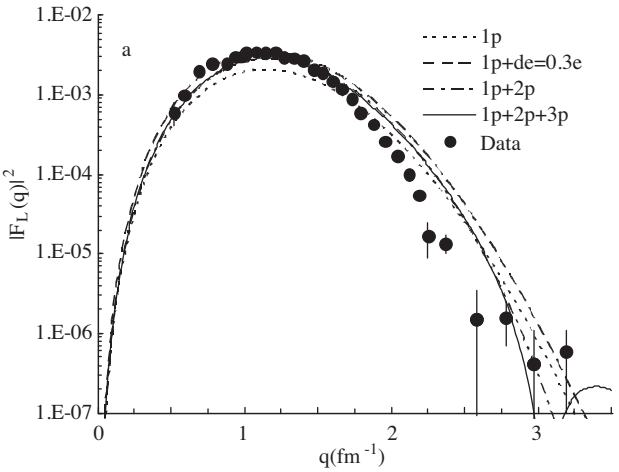


**Figure 5.** C2 form factor for $J^\pi T = \frac{3}{2}^-_1 \frac{1}{2}$ state at $E_X$ =6.32 MeV in $^{15}$**N**. Data are from [28].

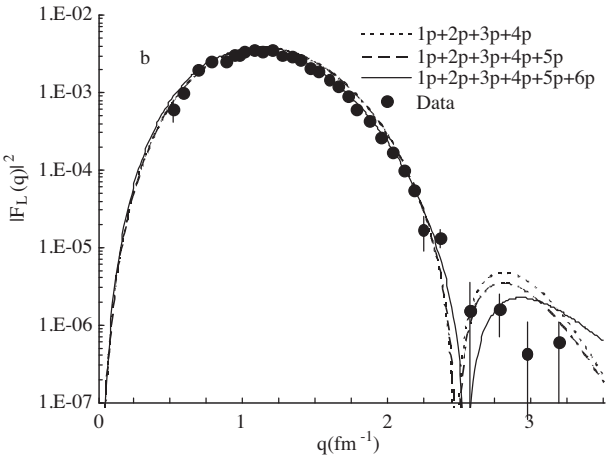


**Figure 6.** C2 form factor for $J^\pi T = \frac{3}{2}^-_1 \frac{1}{2}$ state at $E_X$ =6.32 MeV in $^{15}$**N**. Data is from [28].

Calculations that include microscopic core polarization effects [27] through excitations from the core orbits up to higher orbits with $2\,\hbar\omega$ excitations do not explain this behavior. It appears that such a structure requires the contribution of higher shells.

Mixing in the 2p shell shifted the results of the dashed-dotted curve in Figure 5 towards the experimental value of the minimum diffraction, while a small hump appears at $q > 3\,fm^{-1}$ due to (1p+2p+3p) shells contribution in the initial and final states, as shown in the solid curve of Figure 5.

Consideration of the 4p, 5p, and 6p shells, respectively, in turn influences the C2 form factor as shown in Figure 6 as the dotted, dashed, and solid curves. All these curves show the diffractive structure of this C2 form factor and predict the correct position of the minimum diffraction. However, both the dotted and dashed curves overestimated the data slightly at $1.25\,fm^{-1} < q < 2.1\,fm^{-1}$.

Thus, admixture of the shells (2p+3p+4p+5p+6p) with the 1p shell in the initial and final states give the best description to the data since they have large error bars for that data of the second lobe. The following wave functions are used to calculate the solid curve in Figure 6:

$$|i\rangle = -0.97\,|1p\rangle + 0.1\,|2p\rangle + 0.2\,|3p\rangle - 0.01\,|4p\rangle + 0.01\,|5p\rangle + 0.094\,|6p\rangle\,,$$

$$|f\rangle = 0.97\,|1p\rangle + 0.1\,|2p\rangle - 0.2\,|3p\rangle + 0.01\,|4p\rangle + 0.01\,|5p\rangle + 0.094\,|6p\rangle\,.$$

However, the effective charge model enhances the value of $B(C2\uparrow, q = k)$ predicted by CK model calculations, and the above modification in $|i\rangle$ and $|f\rangle$ retains this enhancement, as explained in Table 1.

Radhi et al. [29] showed that the high $q$ data depend strongly on the radial part of the single-particle wave functions. The high $q$ data for the $J^\pi T(E_X, \mathrm{MeV}) = \frac{1}{2}^-\frac{1}{2}$ (0.478) and $\frac{7}{2}^-\frac{1}{2}$ (4.63) states in $^7$Li and $J^\pi T(E_X, \mathrm{MeV}) = \frac{3}{2}^-\frac{1}{2}(6.32)$ in $^{15}$N were successfully described when the radial part of the single-particle wave functions were those of the Woods-Saxon potential, rather than the harmonic oscillator potential. Their calculations included core-polarization effects. In the present work, the radial part of single particle wave functions of the harmonic oscillator potential, has been modified by including higher shells.

# 4. Conclusions

The truncated model space that include the shells $1p_{3/2}$ and $1p_{1/2}$ only $(0\hbar\omega)$ is less successful for describing the dynamic properties such as electron scattering form factors and reduced transition probabilities in the nuclei of atomic mass $4<A<16$. Extending the model space to include the full $(0+2+4)\hbar\omega$ fail to reproduce the diffractive structures of the experimental C2 form factors of $^7$Li. Consideration of higher-energy excitations up to $6\,\hbar\omega$ through core polarization effects fail also to describe this structure in $^7$Li. Our calculations, which were carried out in the extended space involving admixture of the harmonic oscillator shells (1p+2p+3p) and (1p+2p+3p+4p) in the initial and final wave functions of $^7$Li, reproduce the data excellently. On the other hand, the wave functions of $^{12}$C and $^{15}$N require admixtures of higher shells up to 7p and 6p, respectively, to give the best description for the electron scattering form factors. However, the results of the present work denote that the extension involving such an incomplete multi-$\hbar\omega$ model space may compensate any other effects that interfere destructively with some components of the full multi-$\hbar\omega$ model space calculations. And this may justify the present approach. Another longitudinal and transverse form factors for nuclei in the p- and sd-shell regions are left as subjects for future works in the framework of this approach.

# Acknowledgements

The author would like to express his thank to Prof. Dr. R. A. Radhi, (Physics Department/ Science College/ Baghdad University/ IRAQ) for reading the manuscript and his valuable notes.

# References

[1] S. Cohen and D. Kurath, *Nucl. Phys.*, **73**, (1965), 1.

[2] A. A. Wolters, A. G. M. van Hees and P. W. M. Glaudemans, *Phys. Rev.*, **C42**, (1990), 2053.

[3] A. A. Wolters, A. G. M. van Hees and P. W. M. Glaudemans, *Phys. Rev.*, **C42**, (1990), 2062.

[4] J. G. L. Booten and A. G. M. van Hees, *Nucl. Phys.*, **A569**, (1994), 510.

[5] R. A. Radhi, A. A. Abdullah, Z. A. Dakhil and N. M. Adeeb, *Nucl. Phys.*, **A696**, (2001), 442.

[6] I. Talmi, *Phys. Rev.*, **C39**, (1989), 284.

[7] R. L. Huffman, J. Dubach, R. S. Hicks and M. A. Plum, *Phys. Rev.*, **C35,** (1987), 1.

[8] R. A. Radhi, M. A. Elawi and Z. A. Dakhil, *Indian J. Theo. Phys.*, **48**, (2000), 13.

[9] T. W. Donnelly and I. Sick, *Rev. Mod. Phys.,* **56**, (1984), 461.

[10] L. J. Tassie and F. C. Barker, *Phys. Rev.*, **111**, (1958), 940.

[11] B. A. Brown, B. H. Wildenthal, C. F. Williamson, F. N. Rad, S. Kowalski, H. Crannell and J. T. O'Brien, *Phys. Rev.*, **C32**, (1985), 1127.

[12] T. S. H. Lee and D. Kurath, *Phys. Rev.*, **C21**, (1980), 293.

[13] E. deVries et al., *At. Data Nucl. Data Tables*, **36**, (1987), 500.

[14] J. B. Flanz, R. S. Hicks, R. A. Lindgren, G. A. Peterson, A. Hotta, B. Parker and R. S. York, *Phys. Rev. Lett.*, **41**, (1978), 1642.

[15] C. W. de Jager, H. de Vries and C. de Vries, *At. Data Nucl. Data Tables*, **14**, (1974), 179.

[16] J. G. L. Booten, A. G. M. van Hees, P. W. M. Glaudemans and P. J. Brussaard, *Nucl. Phys.*, **A549**, (1992), 197.

[17] S. Karataglidis, B. A. Brown, K. Amos and P. J. Dortmans, *Phys. Rev.*, **C55,** (1997), 2826.

[18] J. Lichtenstadt, J. Alster, M. A. Moinester, J. Dubach, R. S. Hicks, G. A. Peterson and S. Kowalski, *Phys. Lett.*, **B219**, (1989), 394.

[19] J. Lichtenstadt, J. Alster, M. A. Moinester, J. Dubach, R. S. Hicks, G. A. Peterson and S. Kowalski, *Phys. Lett.*, **B244**, (1990), 173.

[20] R. Yen, L. S. Cardman, D. Kalinsky, J. R. Legg and C. K. Bockelman, *Nucl. Phys.*, **A235**, (1974), 135.

[21] B. T. Chertok, C. Sheffield, J. W. Lightbody, S. Penner and D. Blum, *Phys. Rev.*, **C8**, (1973), 23.

[22] G. A. Beer, D. Brix, H. G. Clerc and B. Laube, *Phys. Lett.*, **B26**, (1986), 506.

[23] U. Deutschmann, G.Lahm, R. Neuhausen and J. C. Bergstrom, *Nucl. Phys.,* **A411**, (1983), 337.

[24] H. Sagawa, T. Suzuki, H. Hyuga and A. Arima, *Nucl. Phys.*, **A322**, (1979), 361.

[25] T. Suzuki, H. Hyuga and A. Arima and K. Yazaki, *Nucl. Phys.*, **A358,**(1981), 421c.

[26] S. Karataglidis, P. J. Dortmans, K. Amos and R. de Swiniarski, *Phys. Rev.*, **C52**, (1995), 861.

[27] R. A. Radhi, *Eur. Phys. J.*, **A16**, (2003), 387.

[28] J. Millener, extracted from ref. [27].

[29] R. A. Radhi, A. K. Hamoudi and K. S.Jassim, *Indian J. Phys.*, **81**, (2007), 683.